The electronic structure of $CaCuO_2$ and $SrCuO_2$

1999 J. Phys.: Condens. Matter 11 4637

(http://iopscience.iop.org/0953-8984/11/24/305)

J. Phys.: Condens. Matter **11** (1999) 4637–4646. Printed in the UK PII: S0953-8984(99)02734-4

The electronic structure of $CaCuO_2$ and $SrCuO_2$

Hua Wu†, Qing-qi Zheng†‡, Xin-gao Gong†§ and H Q Lin‡

† Institute of Solid State Physics, Academia Sinica, PO Box 1129, 230031 Hefei, People's Republic of China

‡ Department of Physics, The Chinese University of Hong Kong, Shatin, NT, Hong Kong, People's Republic of China

§ CCAST (World Laboratory), PO Box 8730, 100080 Beijing, People's Republic of China

Received 17 March 1999, in final form 21 April 1999

Abstract. We have calculated and compared the electronic structures of both the 1D CuO-chain compound $SrCuO_2$ and the 2D CuO_2-plane material $CaCuO_2$, on the basis of the local-spin-density approximation (LSDA) and the on-site Coulomb interaction correction (LSDA + U). The LSDA calculation gives a nonmagnetic and metallic solution as usual for $CaCuO_2$, while it yields an antiferromagnetic (AFM) and insulating one for $SrCuO_2$ due to the decreasing pd hybridization and the subsequent spin polarization with lowering dimensionality. Strongly in favour of orbital and spin polarizations of the Cu 3d states, the U interaction dominates in forming the charge transfer insulating character of both of the AFM cuprates. Some of the differences between the electronic structures can be qualitatively accounted for by the variance of dimensionality.

1. Introduction

Copper oxides have attracted much research interest in recent decades, especially after the discovery of high critical temperature (H-T_c) superconductivity [1]. Most of the known cuprate superconductors share a common structural feature, namely the presence of a 2D CuO_2 plane with antiferromagnetic (AFM) ordering Cu^{2+} ($S = 1/2$) sites. Being a parent material of H-T_c superconductors, $CaCuO_2$ has the most crystallographically simple and common 2D CuO_2-plane structure [2] and has naturally drawn much attention for the reason that investigations of it can be regarded as a guide to the study of H-T_c superconductivity [3–5]. As an elementary aspect, the understanding of the electronic and magnetic properties of $CaCuO_2$ should be addressed. $CaCuO_2$ is an AFM insulator, while a standard band calculation based on the local density functional (LDF) predicts it to be a nonmagnetic (NM) metal [3]. This deviation is commonly ascribed to a deficiency of LDF, that is a general underestimation of on-site Coulomb interactions U typical of this kind of strongly correlated electron system. With an inclusion of the U-correction, a local-density approximation plus U (LDA + U) calculation reproduced its AFM and insulating character [5].

Very recently, the 1D CuO-chain antiferromagnet $SrCuO_2$ stimulated many studies after an experimental observation of spin–charge separation in angle-resolved photoemission spectroscopy (ARPES) [6, 7]. The ARPES data show a distinct 1D behaviour, which is qualitatively different from the ARPES data of 2D $Sr_2CuO_2Cl_2$, and which can be quantitatively accounted for by the t–J model [6, 7]. The two observed low binding energy bands with energy dispersions of about 1.2 and 0.3 eV have been identified as a holon band and a spinon one respectively, and the former is scaled by a hopping term t and the latter by an AFM exchange

0953-8984/99/244637+10$19.50

constant J [6, 7]. The 1D CuO-chains in $SrCuO_2$ are formed by 180° Cu–O–Cu bonds, and they are coupled through suppressed 90° Cu–O–Cu bonds [7, 8]. The intrachain J is estimated to be 2100 ± 200 K [6], while the interchain J' is expected to be smaller than J by at least an order of magnitude, making $SrCuO_2$ an almost ideal system of 1D $S = 1/2$ AFM Heisenberg chains [7]. $SrCuO_2$ is a charge transfer (CT) insulator with a gap of 1.8 eV due to strong dd electron correlations [6, 7], whereas a LDA calculation for the NM state gave a metallic solution, despite the fact it yielded valence band structures in good agreement with ARPES results [8].

The aim of this work is to calculate and compare the electronic structures of $CaCuO_2$ and $SrCuO_2$. Although the band structure of $CaCuO_2$ has been analysed by using the local-spin-density approximation (LSDA) [3] and LDA + U [5], the LSDA + U calculation deserves a re-evaluation for two reasons. First, a definition of the U parameter is a crucial step in a L(S)DA + U calculation, since U usually imposes significant influences on the electronic structure of strongly correlated systems. In the previous calculation for $CaCuO_2$, a choice of $U = 7.5$ eV led to a gap of 2.1 eV [5]. However, in a very recent reformulation of the LDA + U method for a local orbital basis, the values of U were typically only 40–65% as large as those currently in use [9]. In a sense, the calculated gap was probably considerably overestimated due to the choice of the large U. Second, $CaCuO_2$ is an anisotropic ionic system due to its crystal field and the non-closed Cu^{2+} 3d shell, while the atomic sphere approximation (ASA) for charge density and LDA potential was employed in the LDA + U calculation [5]. It has been suggested that the ASA could lead to less accurate results for magnetic compounds than a full potential (FP) scheme [10]. On the other hand, we should design LSDA and LSDA + U calculations for the AFM state of $SrCuO_2$, in view of the fact that the previous LDA calculation [8] for the NM state failed to describe the insulating nature of this strongly correlated antiferromagnet. Furthermore, on the basis of our calculations we can easily compare the electronic structure of 1D $SrCuO_2$ with that of 2D $CaCuO_2$ and investigate the influences of dimensionality.

2. Calculational details

The crystal structure data of $CaCuO_2$ and $SrCuO_2$ are taken from references [2] and [8], respectively. We adopt the linear combination of atomic orbitals (LCAO) band method modified within a FP framework where no shape approximation is made for charge density and potential [10]. The numerical atomic (actually ionic) basis functions are generated iteratively by solving the Hohenberg–Kohn–Sham equation [11] for isolated atoms in a crystal environment [12]. Ca 4s and Sr 5s, Cu 3d4s and O 2s2p orbitals are treated as the valence states in a frozen-core approximation. The Hartree potential is expanded into lattice harmonics up to $L = 4$, and the exchange-correlation potential of the von Barth–Hedin type [13] is used.

One-electron band calculations based on the L(S)DA are practical in describing the electronic structure of many materials, and the U-correction proves useful in elucidating the electronic structure of strongly correlated insulators. However, the L(S)DA + U method has the same difficulty as many-body approaches in the tight-binding Hamiltonian because it does not provide an unambiguous way of treating the U term to which many important effects of strong correlations are related. Although there has been considerable progress in first-principle methods for an evaluation of model parameters by using the L(S)DA, an estimation of U involves the problem of how well the constraint L(S)DA works in describing the screening process in solids and the problem of how one can define local orbitals in strongly hybridized systems. Consequently, in many cases the U value has been determined not from first principles but empirically. Thus, a true first-principle approach to strongly correlated systems is still lacking, even on the mean-field level [14]. In addition, the L(S)DA + U method may be

oversimplified regarding a treatment of many-body problems and hence gives less satisfactory descriptions for some details of the electronic structure of strongly correlated systems.

Nevertheless, the L(S)DA+U method provides a practical way of incorporating electronic correlations into first-principle calculations on the Hartree–Fock level. In the following LSDA+U calculations, we adopt the expression [12, 15] of the U-corrected potential dependent on m-orbital and σ-spin of the Cu 3d states

$$V_{m\sigma}^{LSDA+U} = V^{LSDA} + U\sum_{m'}(n_{m'-\sigma} - n^0) + U\sum_{m'(\neq m)}(n_{m'\sigma} - n^0) - I\sum_{m'(\neq m)}(n_{m'\sigma} - n_\sigma^0).$$

$U = 5$ eV is chosen in our calculations, in view of the very recent proposal that the calculated value of U defined on a local orbital basis set varies from 2.7 to 5.1 eV along transition metal monoxides from VO to NiO [9]. This choice, of course, is not absolute, but appropriate as indicated below. The Stoner parameter I is usually smaller than U by nearly an order of magnitude, thus imposing a relatively weak influence upon the electronic states, and it varies at least not strongly for different transition metal oxides [5]. In this work, the previously calculated value for $CaCuO_2$, $I = 0.98$ eV [5], is used for both of the cuprates. The present U-correction accounts well for the CT insulating behaviour of $CaCuO_2$ and $SrCuO_2$, as will be seen below.

3. Results and discussion

For the AFM insulator $CaCuO_2$, the LSDA calculation converges at a NM metallic solution (see figure 1(a)) as usual, except that the present O 2p valence bands lie lower by 1–2 eV than those obtained from a FP linearized-augmented-plane-wave (LAPW) calculation [3]. This strong contradiction calls for an improvement, and the U-correction will be included below. The difference regarding the O 2p bands is most likely due to the present choice of an ionic basis set in the crystal environment instead of the previous [3] neutral basis set. A similar case occurs in the electronic structure calculations for NiO [12, 16] and $CuGeO_3$ [10]. It is well known that a strong hybridization between the Cu $d_{x^2-y^2}$ and O p_x/p_y orbitals in the ab plane suppresses the spin polarization of the $d_{x^2-y^2}$ orbital and forms a wide half-filled conduction band with dispersional width of about 4 eV. It can be seen in figure 2(a) that the pd bonding–antibonding splitting is $\sim$5 eV, which could be a common value in 2D CuO_2-plane compounds [17].

In contrast, the LSDA calculation for the AFM state of $SrCuO_2$ yields an insulating solution with a spin-splitting gap of 0.55 eV, as seen in figures 3(a) and 4(a). The Cu 3d bands and the O 2p bands exhibit a narrow structure. In particular, the two highest valence bands and the two lowest conduction ones, both of which primarily consist of Cu $d_{3z^2-r^2}$ and in-chain O(1) 2p orbitals, appear rather flat along the ab plane perpendicular to the $\vec{c}$-axis CuO(1) chain but look dispersive along the chain direction, indicating the 1D property of $SrCuO_2$ [6–8]. The four bands would merge into two half-filled conduction bands with a dispersional width of about 2 eV, provided that the NM state is assumed. The expected conduction bands agree well with those given by a very recent FP-LAPW calculation [8], and the band width is half that of 2D $CaCuO_2$, which is consistent with a prediction from the tight-binding model.

Owing to the lowering of dimensionality, the in-chain pd hybridization in the $SrCuO_2$ becomes weaker than the in-plane one in $CaCuO_2$, as has been implied by the reduction of band width. As a result, the spin polarization of the d orbitals occurs in $SrCuO_2$, as is reflected by the present calculation which gives a spin moment of 0.33 μ_B carried mainly by the $d_{3z^2-r^2}$ orbital. Thus, the spin density around the Cu^{2+} ion appears nonspherical: higher over the $d_{3z^2-r^2}$ orbital but lower over other d orbitals. The resulting anisotropic exchange potential imposes different influences on the d orbitals by generating the strongly

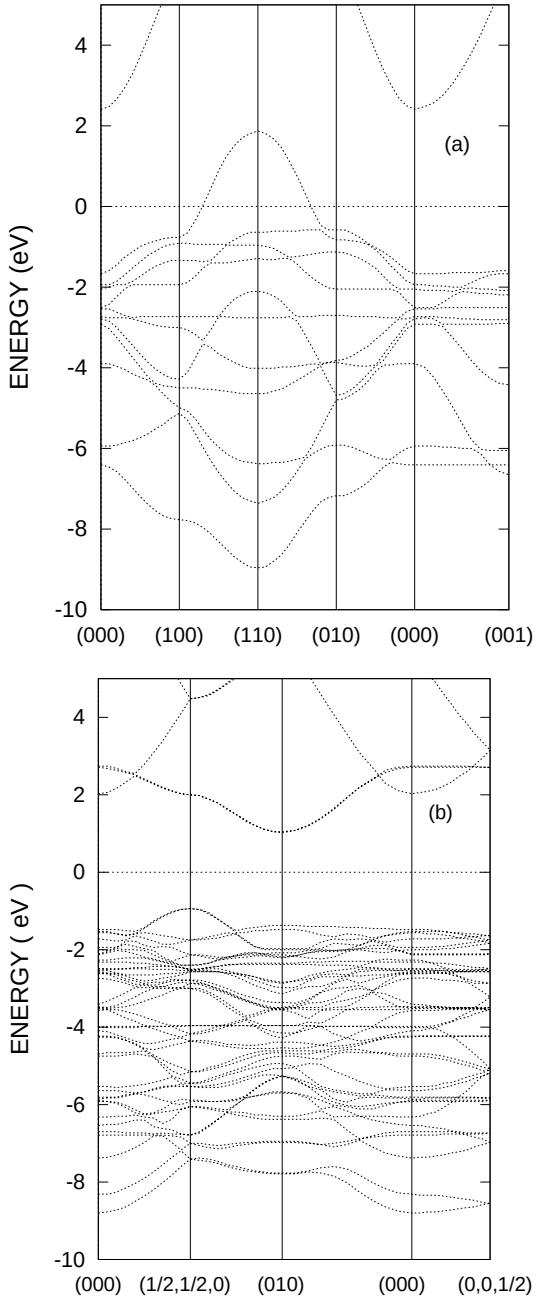

Figure 1. Band structure of $CaCuO_2$ calculated by (a) LSDA: a NM metallic solution and (b) LSDA + U: an AFM insulating state. A $\sqrt{2}a \times \sqrt{2}a \times 2c$ magnetic cell is adopted (see figure 2 in [2]), and the $\vec{k}$ points in the irreducible Brillouin zone (BZ) are expressed in units of (π/a, π/a, π/c). Note that the AFM ordering leads to the folding-up of BZ.

orbital-dependent exchange splittings [10]: 0.68, 0.43 and 0.27 eV for the $d_{3z^2-r^2}$, $d_{x^2-y^2}$ and other d orbitals respectively. Consequently, the enhanced exchange splitting of the

$d_{3z^2-r^2}$ orbital induces the present AFM insulating solution, which qualitatively accords with the experimental one.

The U-correction should be included for the reasons indicated above, i.e. that the LSDA fails to describe the insulating character of $CaCuO_2$ and that the LSDA results for $SrCuO_2$ do not agree with the experimental data.

For $CaCuO_2$, the U interaction opens a large gap of 1.96 eV, which is comparable to the experimental value of 1.5 eV [4]. It can be seen in figure 1(b) that the folding-up of Brillouin zone (BZ) as a result of AFM ordering leads to a change of the positions of both the valence band maximum and the conduction band minimum in reciprocal space. The U repulsion favours orbital and spin polarizations strongly, as is reflected by the result shown in figure 2(b) that the occupied d bands shift down but the unoccupied minority-spin $d_{x^2-y^2}$ band moves up. In particular, the upper Hubbard band and the lower band derived from the $d_{x^2-y^2}$ orbital have an energy separation of $\sim$8 eV, which, aided by the pd bonding–antibonding splitting [17], is larger than the adopted $U = 5$ eV. The resulting spin-polarized $d_{x^2-y^2}$ orbital carries a spin moment of 0.71 μ_B, which, owing to the finite pd hybridization, is smaller than an ideal value of 1 μ_B for the $S = 1/2$ Cu^{2+} ion, but which is larger than the experimental one of 0.51 μ_B [2] reduced by quantum fluctuations [1]. In addition, the remarkable moving down of the occupied d bands leads to an increase of the O 2p component up to 68% at the topmost valence band, thus supporting the proposal of a CT insulator for $CaCuO_2$ [4].

In contrast to the previous calculation where the adoption of $U = 7.5$ eV for $CaCuO_2$ led to a gap of 2.1 eV [5], the present calculation (with a choice of U smaller by one third) gives a slightly smaller gap. Similarly, a recent LCAO-LSDA + U calculation for NiO with $U = 5.4$ eV [12], like the case of $U = 8$ eV [5], accounted for AFM insulating behaviour well. This leads us to the belief that the present choice of U is appropriate for the LCAO basis set. The present spin moment is a little larger than the previous one of 0.66 μ_B [5], as could be ascribed to the contribution of spin polarization induced by the nonspherical exchange potential around the Cu^{2+} ion [10]. Note that the definition of the spin moment depends on the choice of atomic radii [16] and the basis set to some extent.

For $SrCuO_2$, the U-correction increases the gap and the spin moment up to 2.36 eV and 0.71 μ_B respectively. The U interaction lowers the $d_{3z^2-r^2}$ valence band and results in a reduction of the 3d component down to 45% but an increase of the 2p one up to 55% at the topmost valence band, leading us to classify this cuprate as a CT insulator rather than a Mott–Hubbard one. The calculated valence band structures agree well with the ARPES data [7, 8], except for the observed low-binding spinon band. First, the topmost valence band with a maximum at the Z $(0, 0, \pi/2c)$ point has a dispersional width of 0.6 eV between Γ $(0, 0, 0)$ and Z along the $\vec{c}$-axis CuO(1)-chain direction, which agrees with the observed holon-band feature in the same region [7]. This is expected since the motion of a hole should be determined by t, which a band calculation should predict very well [7]. Next, the narrow Cu 3d and O 2p valence bands are distributed densely over a range of energy from binding energy $E_b = 1.5$ to 7 eV, as seen in figures 3(b) and 4(b). Along the Γ–X ($\vec{a}$-axis) direction, for example, these bands could be divided into three groups, lying above $E_b = 2$ eV, between 2.5 and 4.5 eV, and below 5 eV. The three groups of bands have counterparts in the ARPES data along the $\vec{a}$-axis direction [8]. Finally, although the ARPES structures along the $\vec{c}$-axis direction appear complicated [8], assignments of them could be made by the present calculation. The dispersive bands at the bottom of the ARPES structures are attributed to the bonding states formed mainly by the $d_{3z^2-r^2}$ and the in-chain O(1) 2p orbitals. The measured bands around $E_b = 6$ eV may be ascribed to the states hybridized between the 't_{2g}' (xy, xz, yz) and the O(1)/O(2) 2p orbitals. Also, the observed structures at $E_b = 2$–4 eV could be assigned to

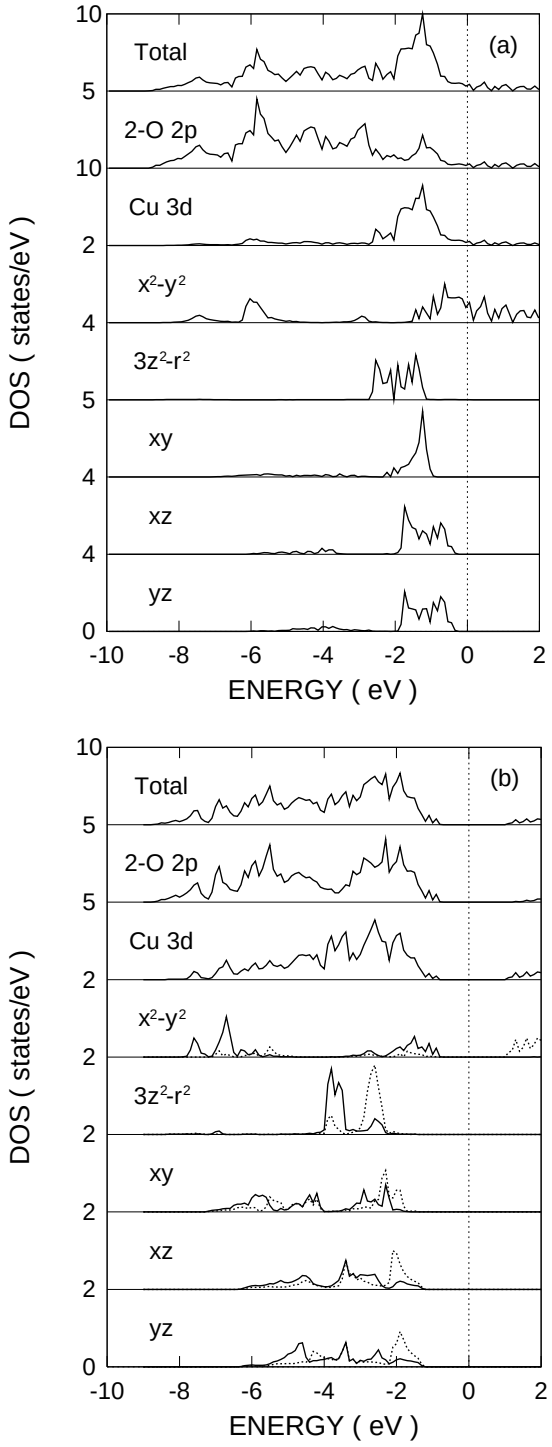

Figure 2. Total density of states (DOS) per formula and projected DOS for (a) the NM metallic state of $CaCuO_2$ and (b) the AFM insulating state. (b) The U interaction modifies the Cu 3d bands remarkably. For the 3d projected DOS, the solid (dashed) curve denotes the majority (minority) spin.

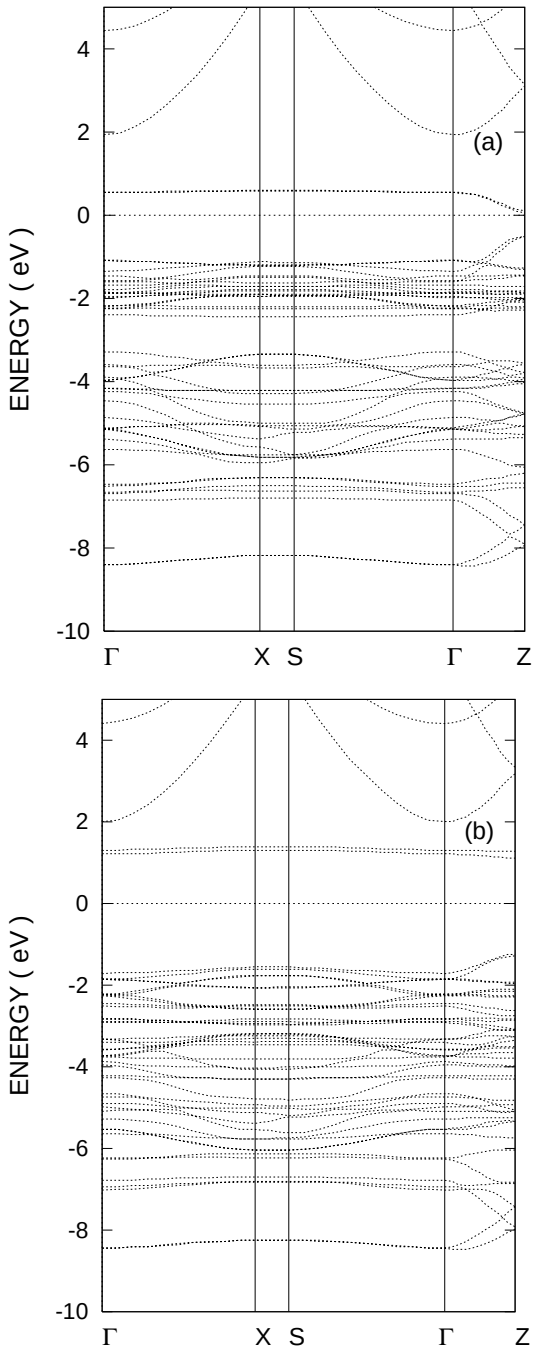

Figure 3. Band structure of $SrCuO_2$ calculated by (a) LSDA and (b) LSDA + U. The ΓXSΓ directions in the *ab* plane are perpendicular to the ΓZ direction parallel to the $\vec{c}$-axis CuO-chain.

more pd hybridized states. The analyses above are consistent with the previous ones made from a FP-LAPW calculation [8].

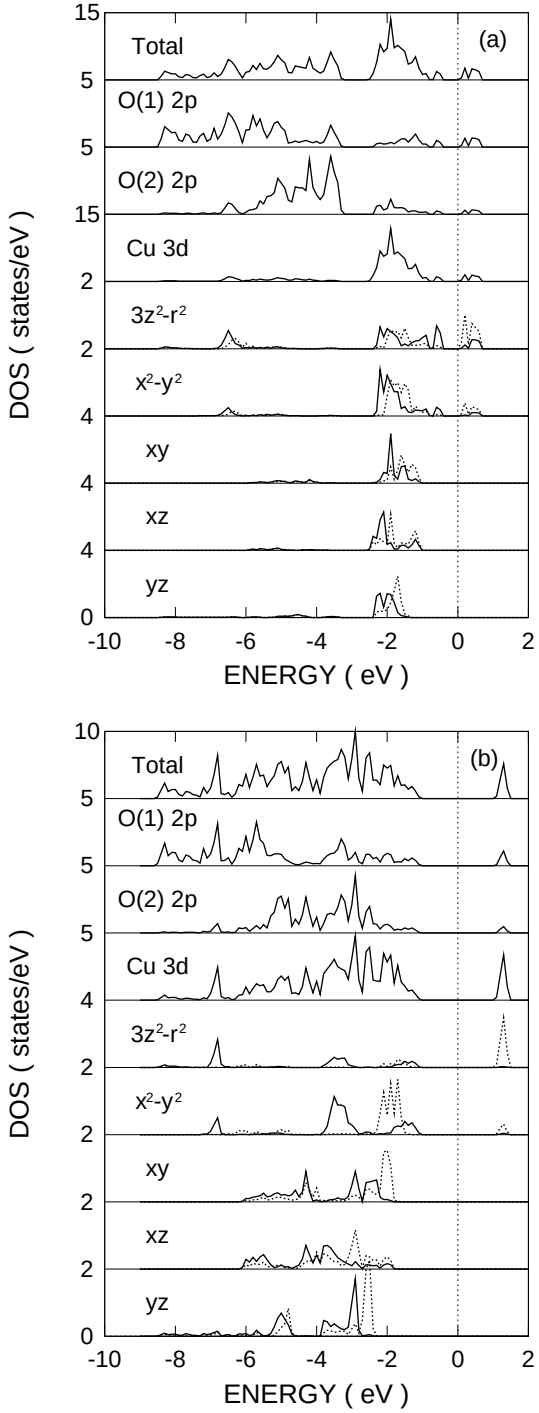

Figure 4. Total DOS per formula and projected DOS for $SrCuO_2$ calculated by (a) LSDA and (b) LSDA + U. O(1) and O(2) represent the in-chain oxygen and the apical one respectively (see figure 1 in [8]). For the 3d projected DOS, the solid (dashed) curve denotes the majority (minority) spin. (a) The enhanced exchange splitting of the $d_{3z^2-r^2}$ orbital induces the AFM insulating solution. (b) The U interaction increases the gap considerably.

Our calculations have successfully reproduced the CT insulating behaviour of 2D $CaCuO_2$ and 1D $SrCuO_2$. Here, we compare the calculated values of the gap for both of the cuprates. On the one hand, the two values are comparable, as is to be expected since the same U parameter is adopted for the on-site Coulomb interaction which primarily determines the size of the gap. On the other hand, according to experimental measurements [4, 6], the calculated gap for $CaCuO_2$ is a little smaller than that for $SrCuO_2$, partly attributable to the lowering of dimensionality from 2D to 1D and thus to the reduction of band width. It is not surprising that the LSDA + U calculations give an identical spin moment of 0.71 μ_B for $CaCuO_2$ and $SrCuO_2$, in view of the important role played by the U interaction. Owing to quantum fluctuations which behave more strongly in 1D spin systems than in 2D ones [18], however, the actual spin moment in $SrCuO_2$ is most likely smaller than that (0.51 μ_B [2]) in $CaCuO_2$, and it is expected to be of the same order of magnitude as 1D Sr_2CuO_3 with a spin moment estimated to be less than 0.1 μ_B [18].

4. Conclusion

We have investigated the electronic structures of 1D $SrCuO_2$ and 2D $CaCuO_2$ by performing LSDA and LSDA + U calculations. We summarize as follows. (1) The strong pd hybridization in the 2D CuO_2-plane favours a NM metallic solution for $CaCuO_2$, while the decreasing pd hybridization in the 1D CuO-chain and the subsequent spin polarization lead to an AFM insulating state for $SrCuO_2$. (2) The on-site dd electron correlations, splitting the half-filled d band remarkably, open a large gap for $CaCuO_2$ and increase the gap for $SrCuO_2$ considerably. (3) Some of the electronic structure differences between $SrCuO_2$ and $CaCuO_2$ can be qualitatively accounted for by the variance of dimensionality. The present work reproduces the CT insulating nature of both the AFM cuprates well.

Acknowledgments

One of the authors, H Wu, would like to thank L J Zou and Z Zeng for their valuable suggestions. This work was supported by the PanDeng Project 95-YU-41 and the NSF of China (19574057), and it was financed by CAS (LWTZ-1298).

References

[1] Pickett W E 1989 *Rev. Mod. Phys.* **61** 433
[2] Vaknin D, Caignol E, Davies P K, Fischer J E, Johnston D C and Goshorn D P 1989 *Phys. Rev.* B **39** 9122
[3] Singh D, Pickett W E and Krakauer H 1989 *Physica* C **162–164** 1431
[4] Tokura Y, Koshihara S, Arima T, Takagi H, Ishibashi S, Ido T and Uchida S 1990 *Phys. Rev.* B **41** 11 657
[5] Anisimov V I, Zaanen J and Andersen O K 1991 *Phys. Rev.* B **44** 943
[6] Kim C, Matsuura A Y, Shen Z-X, Motoyama N, Eisaki H, Uchida S, Tohyama T and Maekawa S 1996 *Phys. Rev. Lett.* **77** 4054
[7] Kim C, Shen Z-X, Motoyama N, Eisaki H, Uchida S, Tohyama T and Maekawa S 1997 *Phys. Rev.* B **56** 15 589
[8] Nagasako N, Oguchi T, Fujisawa H, Akaki O, Yokoya T, Takahashi T, Tanaka M, Hasegawa M and Takei H 1997 *J. Phys. Soc. Japan* **66** 1756
[9] Pickett W E, Erwin S C and Ethridge E C 1998 *Phys. Rev.* B **58** 1201
[10] Wu H, Qian M C and Zheng Q Q 1999 *J. Phys.: Condens. Matter* **11** 209
[11] Hohenberg P and Kohn W 1965 *Phys. Rev.* B **136** 864
Kohn W and Sham L J 1964 *Phys. Rev.* A **140** 1133
[12] Hugel J and Kamal M 1997 *J. Phys.: Condens. Matter* **9** 647
[13] von Barth U and Hedin L 1972 *J. Phys. C: Solid State Phys.* **5** 1629
[14] Imada M, Fujimori A and Tokura Y 1998 *Rev. Mod. Phys.* **70** 1039

[15] Pan Wei and Zheng Qing Qi 1994 *Phys. Rev.* B **49** 10 864
Pan Wei and Zheng Qing Qi 1994 *Phys. Rev.* B **49** 12 159
[16] Terakura K, Oguchi T, Williams A R and Kübler J 1984 *Phys. Rev.* B **30** 4734
[17] Czyzyk M T and Sawatzky G A 1994 *Phys. Rev.* B **49** 14 211
[18] Ami T, Crawford M K, Harlow R L, Wang Z R, Johnston D C, Huang Q and Erwin R W 1995 *Phys. Rev.* B **51** 5994